Volodymyr Bereziuk[1], Yaroslav Sokolovskyy[2]

[1] Computer Science Department, National Forestry University of Ukraine, Henerala Chuprynky street, 103, Lviv, Ukraine, E-mail: volodymy.berezyuk@nltu.edu.ua, ORCID 0009-0001-6930-4235
[2] Computer Design Systems Department, Lviv Polutechnic National University,S. Bandery street 12, Lviv, Ukraine, E-mail: yaroslav.i.sokolovskyi@lpnu.ua, ORCID 0000-0003-4866-2575

ENHANCEMENT OF MEDICAL MRI IMAGES BASED ON THE ATANAGAN-BALEANU FRACTAL OPERATOR

Abstract. This article describes the use of the Atangana-Baleanu fractal operator for the task of enhancing textures in medical MRI images. It provides a detailed explanation of the mathematical framework of the Atangana-Baleanu fractal differential. A numerical approach for calculating the fractal differential using the finite difference method is considered. Based on the approximated solution, approximation coefficients are determined. These coefficients are used to create eight differently oriented masks, which serve as filters for spatial image processing in various directions. A corresponding algorithm for applying fractal masks is developed and described. The obtained results of the algorithm's performance on medical image processing are compared. The impact of the image enhancement algorithm on image parameters is also investigated. Furthermore, a comparison with other texture enhancement algorithms is conducted.

Introduction

Medical images are an integral part of diagnosing and treating patients, as they allow doctors to visualize the internal structures of organs and tissues without the need for surgical intervention. They enable the detection of diseases at early stages, monitor treatment effectiveness, and plan future surgeries. It is crucial for doctors that these images are as clear and detailed as possible, as this significantly enhances diagnostic accuracy and helps in selecting the optimal treatment approach.

One of the most widely used methods of medical imaging is Magnetic Resonance Imaging (MRI) of the brain. It produces detailed images of brain tissues using a magnetic field and radiofrequency pulses. However, MRI also has certain drawbacks: noise and artifacts can affect images, and the smallest structures may sometimes lose clarity. These limitations can make it challenging to establish an accurate diagnosis.

To overcome these limitations, computer-based image processing methods are used, which help make the texture of MRI images more detailed and comprehensible. By applying various techniques to enhance textures and increase contrast, the fine details of brain structures become clearer and easier to analyze. Among modern approaches, a method that uses the fractal differential for texture enhancement stands out. This approach, based on the principles of fractal mathematics, allows for flexible enhancement of complex details that exhibit self-similarity. Fractal operators have a unique ability to operate across different scales, which aids in analyzing and emphasizing the smallest elements of an image. While traditional methods have limitations in reproducing the finest details, fractal processing can highlight these elements without losing clarity, making the images more informative and accurate for clinical purposes.

Problem statement

The object of the study is the textures of medical images produced by MRI. The subject of the study

is the algorithms and methods for enhancing MRI image textures using fractal derivatives. The objective of the work is to apply the mathematical framework of the Atangana-Baleanu fractal operator and develop algorithmic and software tools for enhancing the textures of medical MRI images of the brain. To achieve this goal, the following sub-tasks can be identified:

• To examine the theoretical foundations of the Atangana-Baleanu fractal derivative.

• To develop an algorithm for enhancing image textures using the fractal derivative.

• To create a software implementation of the texture enhancement algorithm.

• To conduct visual and numerical studies to assess the effectiveness of the developed algorithm.

• To compare the results of texture enhancement using the fractal derivative with other conventional methods.

• To analyze the obtained results and draw conclusions about the feasibility of using the Atangana-Baleanu fractal derivative for image texture enhancement.

The scientific novelty of the work lies in the adaptation of an algorithm for enhancing medical MRI image textures using the Atangana-Baleanu fractal derivative.

The practical significance of the work is in the application of software and algorithmic tools for enhancing medical MRI image textures using the Atangana-Baleanu fractal derivative. The use of this method will improve the textures of MRI images, which will contribute to more accurate disease diagnosis, facilitate the identification and analysis of small brain structures, and enhance the effectiveness of treatment planning and surgical interventions.

Review of Modern Information Sources on the Subject of the Paper

Existing image texture enhancement methods play an important role in processing complex structures, particularly in medical diagnostics. Various techniques are commonly used to enhance texture features, detect edges, and improve contrast. The main approaches include nonlinear transformation methods (Laplace pyramid) [1], wavelet transformation [2], filters based on derivatives of integer orders (Prewitt, Sobel) [3, 4], fractal methods [5], and others. Each approach has its unique properties and limitations.

Methods based on nonlinear transformations, such as the Laplace pyramid, create multi-level representations of an image, allowing the processing of different frequency regions. They are suitable for texture enhancement by amplifying details, but they can cause artifacts and distortions in the form of artificial contours, especially in areas with smooth brightness transitions. Wavelet transformation is used for analyzing and enhancing various frequency components, helping to achieve sharper textures. However, it may not retain enough information in low-frequency regions, leading to the loss of important low-frequency structures. Filters based on derivatives of integer orders are commonly used to detect edges and high-frequency components of an image. However, these methods struggle to correctly process textures on complex and irregular surfaces, especially under low contrast conditions, which are typical for medical images.

MRI visualization enables the acquisition of high-quality images of the brain's internal structures. However, MRI images often suffer from low contrast and the presence of artifacts, especially within fine and high-frequency structures. Additionally, MRI images are prone to signal inhomogeneity and exhibit varying intensities in different areas, making it difficult to highlight small structures. The main issues affecting the quality of MRI images include low contrast between neighboring tissues, signal inhomogeneity, and poor definition of high-frequency details. These challenges complicate the extraction of details critical for diagnosis. Texture enhancement helps to increase the contrast of small structures and improve the clarity of boundaries between different tissue types, which is crucial for anatomical analysis and early diagnosis.

Fractal methods are a promising approach for texture enhancement, especially in MRI images, due to their ability to emphasize high-frequency components while preserving information about low-frequency regions. Fractal methods utilize the self-similarity of texture to process various frequency components of an image, allowing for effective extraction of even irregular and complex textures. The fractal properties of natural structures (including brain tissue) enable the effective highlighting of

characteristic irregular details. In the context of MRI images of the brain, where it is important to preserve information about low-frequency regions (such as the boundaries of different tissues) while simultaneously improving the visibility of high-frequency details, fractal methods have a significant advantage. Due to their ability to enhance details of different sizes equally well, these methods allow for precise identification of boundaries and contours while maintaining the overall structure of the image.

In the article [6], the creation of fractal differential masks, including YuiFeiPU2 based on the Grünwald-Letnikov fractal operator, is described. In article [7], the Atangana-Baleanu fractal differential is discussed. The Atangana-Baleanu fractal differential is used to describe complex natural and artificial processes that possess both local and global properties. The Atangana-Baleanu model includes infinite memory and long-term dependence—two properties that are important for systems where the current state depends not only on the present time but also on the entire history of changes. The Mittag-Leffler function, which serves as the kernel in the Atangana-Baleanu operator, better reflects complex natural phenomena and does not have the strict locality constraints that are present in the usual exponential function. The Atangana-Baleanu fractal operator has already been used for image processing, as seen in references [8, 9], which discuss the approximation of the Atangana-Baleanu integral and the creation of masks for edge enhancement and noise reduction in images.

Objectives and Problems of Research

The article [10] describes the approximation of the Atangana-Baleanu fractal differential using the finite difference method. A review of the literature reveals that there are no studies on the application of the mathematical framework of the Atangana-Baleanu fractal operator for processing medical MRI scans of the brain in the context of comparison with other algorithms. This work is dedicated to reviewing the Atangana-Baleanu fractal differential, its approximation, and the adaptation of algorithms and software for processing medical MRI images of the brain.

Main Material Presentation

In this section, a review of fractal operators for derivatives is provided: Grünwald-Letnikov, Riemann-Liouville, Caputo, Atangana-Baleanu, and others [11].

The Grünwald-Letnikov fractional derivative can be expressed as:

$$D_{G\text{-}L}^{v} S(x) = \frac{d^{v}}{[d(x-a)]^{v}} s(x)_{G-L} = \lim_{N \to \infty} \left\{ \frac{\frac{x-a}{N}}{\Gamma(-v)} \sum_{k=0}^{N-1} \frac{\Gamma(k-v)}{\Gamma(k+1)} * s\left(x - k\left(\frac{x-a}{N} \right) \right) \right\},$$ (1)

where $D_{G\text{-}L}^{v}$ - Grunwald-Letnikov fractional differential operator, for signal s(x) in between [a,x], v- any real number (including fractional), Γ – gamma function.

Caputo's fractional derivative can be expressed as:

$$D_{C}^{v} S(x) = \frac{1}{\Gamma(n-v)} \int_{a}^{x} \frac{s^{(n)}(t)}{(x-t)^{v-n+1}} dt,$$ (2)

where D_{c}^{v} - the Caputo fractional differential operator, for signal s(x) in between [a,x], of order v, $s^{(n)}(t)$ classical n-th derivative s(t).

The Atangana-Belean fractional derivative in the context of Caputo (ABC) [7] can be expressed as:

$$D_{ABC}^{v} S(x) = \frac{M(v)}{1-v} \int_{a}^{x} S'(t) E_{v}\left(-v \frac{(x-t)^{(v)}}{1-v} \right) dt,$$ (3)

where D_{ABC}^{v} - fractional derivative of Atangana-Beleanu, for signal s(x) in between [a,x], of order v. M(v) – is a normalization function, E_{v} -Mittag-Leffler function, $s'(t)$ classical derivative of a function s(t).

The Mittag-Leffler function is expressed as:

67

$$E_v(x) = \sum_{k=0}^{x} \frac{x^k}{\Gamma(vk+1)} . \tag{4}$$

The normalization function M(v)is expressed as:

$$M(v) = 1 - v + \frac{v}{\Gamma(v)} . \tag{5}$$

To construct a fractal differential mask for image processing, it is necessary to determine the mask coefficients. This section describes the numerical approximation of the expression (3) of the Atangana-Baleanu fractional differential. In article [10], numerical approximations are performed using the backward finite difference method (FDM). In our case, it was decided to use the central finite difference scheme. This method allows determining the value of the derivative at a specific point based on the function values at the next and previous points. The calculation formula involves the difference between the function values at the previous and next points, divided by two approximation steps.:

$$\frac{dy}{dx} = \frac{y^{i+1} - y^{i-1}}{2\Delta x} \tag{6}$$

Using the discretization techniques from article [10], let the signal S(x) be discretized into L equal parts $x_1, x_2 \dots x_L$ in the interval [0, x]. Then, the L+1 parts of the signal can be written as follows:

$$S_L = S(0)$$

$$...$$

$$S_k = S(x - kx/L) , \tag{7}$$

$$...$$

$$S_0 = S(x)$$

The numerical approximation of operator (3), according to the discretization described in formula (7), will have the following form:

$$\begin{aligned} D_{ABC}^V S(x) &= \frac{M(v)}{1-v} \int_0^x \frac{d}{dx} s(x-t) E_v\left(-v\frac{(t)^v}{1-v}\right) dt \\ &= \frac{M(v)}{1-v} \left[\sum_{k=0}^{L-1} \int_{\frac{kx}{L}}^{\frac{kx+x}{L}} \frac{d}{dx} s(x-t) E_v\left(-v\frac{(t)^v}{1-v}\right) dt \right] \end{aligned} , \tag{8}$$

To calculate the first-order differential in formula (8), we will use the central finite difference scheme (6), then the integrand will be transformed using the Newton-Leibniz formula:

$$\begin{aligned} &\int_{\frac{kx}{L}}^{\frac{kx+x}{L}} \frac{d}{dx} s(x-t) E_v\left(-v\frac{(t)^v}{1-v}\right) dt \\ &= \frac{s(x+x/L) - s(x-x/L-kx/L)}{2(x/L)} \int_{\frac{kx}{L}}^{\frac{kx+x}{L}} E_v\left(-v\frac{(t)^v}{1-v}\right) dt \\ &= \frac{s_{k-1} - s_{k+1}}{2(x/L)} \int_{\frac{kx}{L}}^{\frac{kx+x}{L}} E_v\left(-v\frac{(t)^v}{1-v}\right) dt \\ &= \frac{s_{k-1} - s_{k+1}}{2} \left\{ (k+1) E_{v,2}\left[-\lambda(k+1)^v \left(\frac{x}{L}\right)^v \right] \right. \\ &\left. - k E_{v,2}\left[-\lambda k^v \left(\frac{x}{L}\right)^v \right] \right\} \end{aligned} , \tag{9}$$

where $\lambda = v/1 - v$ i $E_{v,2}$ - the two-parameter Mittag-Leffler function $E_{\alpha,\beta}(x) = \sum\limits_{k=0}^{\infty} \dfrac{x^k}{\Gamma(\alpha k + \beta)}$,where value $\beta = 2$.

Substituting the integral expression from formula (9) into (8), we get:

$$
\mathrm{D}_{\mathrm{ABC}}^{V} S(x) = \frac{M(v)}{1-v} \left\{ \sum_{k=0}^{L-1} \left(\frac{s_{k-1} - s_{k+1}}{2} \right) \right.
$$
$$
\left\{ (k+1) E_{v,2} \left[-\lambda(k+1)^v \left(\frac{x}{L} \right)^v \right] \right. \qquad ,
$$
$$
\left. - k E_{v,2} \left[-\lambda k^v \left(\frac{x}{L} \right)^v \right] \right\}
$$

(10)

The approximated L+1 differences can be written as follows:

$$
\mathrm{D}_{\mathrm{ABC}}^{V} S(x) = \frac{M(v)}{2(1-v)} E_{v,2}(-\lambda h^v) s(x)
$$
$$
+ \frac{M(v)}{2(1-v)} \left[2E_{v,2}(-\lambda 2^v h^v) - E_{v,2}(-\lambda h^v) \right] s(x-h)
$$
$$
+ \frac{M(v)}{2(1-v)} \left\{ \sum_{k=2}^{L-1} (k+1) E_{v,2}(-\lambda(k+1)^v h^v) \right. \qquad ,
$$
$$
- k E_{v,2}(-\lambda k^v h^v)
$$
$$
- (k-1) E_{v,2}(-\lambda(k-1)^v h^v)
$$
$$
\left. + (k-2) E_{v,2}(-\lambda(k-2)^v h^v) s(x-kh) \right\}
$$

(11)

where h=t/L. Expression (11) can be rewritten to the following compact form:

$$
\mathrm{D}_{\mathrm{ABC}}^{V} S(x) = \frac{M(v)}{2(1-v)} \sum_{k=0}^{L} C(k) s(x-kh) ,
$$

(12)

where C(k) filter coefficient, which can be calculated using the formula:

$$
C(k) \begin{cases} E_{v,2}(-\lambda h^v), k = 0 \\[2mm] 2E_{v,2}(-\lambda 2^v h^v) - E_{v,2}(-\lambda h^v), k = 1 \\[2mm] \{ (k+1) E_{v,2}(-\lambda(k+1)^v h^v) \\ - k E_{v,2}(-\lambda k^v h^v) \\ - (k-1) E_{v,2}(-\lambda(k-1)^v h^v) \\ + (k-2) E_{v,2}(-\lambda(k-2)^v h^v) s(x-kh) \}, 1 < k < L \end{cases}
$$

(13)

To process an image, where each pixel has its own finite color value and a specific position in the matrix, masks are used. Considering the function f as the image function with two parameters for the coordinates x and y, the expression for processing along the coordinates x and y can be written as follows:

$$^{x}\mathrm{D}^{v}f(x,y) = C_{0}f(x,y) + C_{1}f(x-1,y) + C_{2}f(x-2,y) + ...$$
$$^{y}\mathrm{D}^{v}f(x,y) = C_{0}f(x,y) + C_{1}f(x,y-1) + C_{2}f(x,y-2) + ... \quad , \tag{14}$$

Based on the expressions from (14), we will construct eight masks with coefficients C(0) … C(L-1) for image processing. According to [6] they will have the following form:

a)   b)   c)   d)

e)   f)   g)   h)
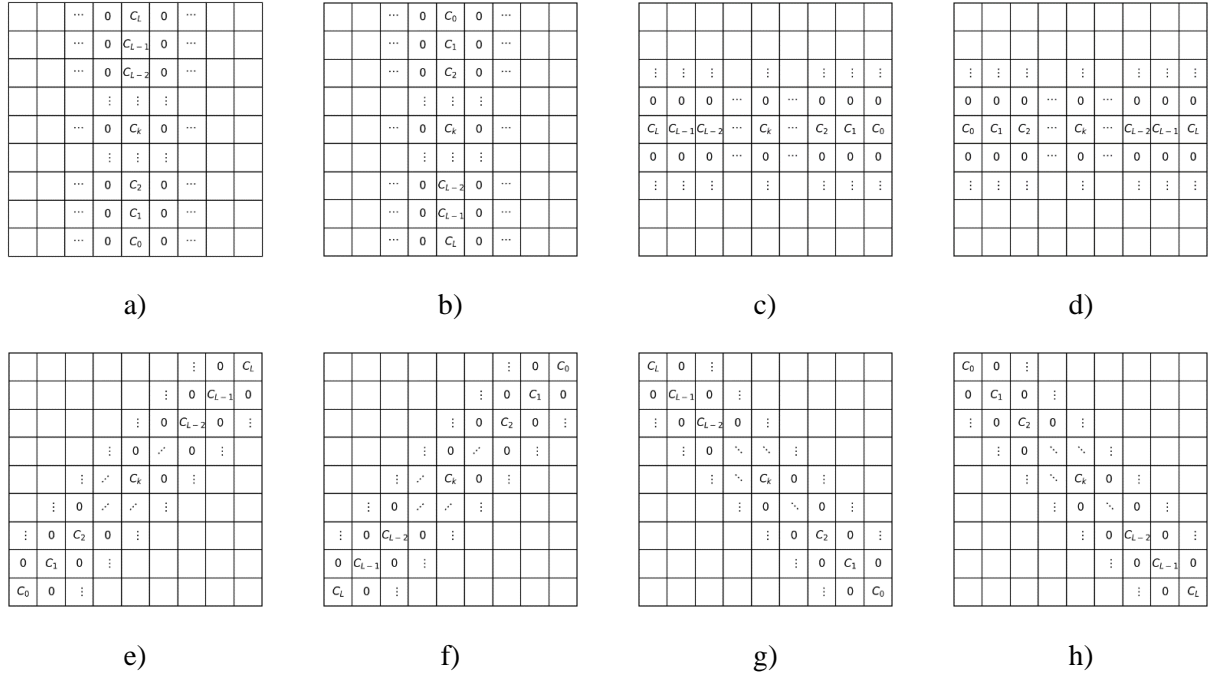
Fig. 1. Fractal differential masks for the eight directions: (a) W1 negative along the x-axis; (b) W2 positive along the x-axis; (c) W3 negative along the y-axis; (d) W4 positive along the y-axis; (e) W5 left ascending diagonal; (f) W6 right descending diagonal; (g) W7 right ascending diagonal; (h) W8 left descending diagonal

Each coefficient C(k) corresponds to a pixel on the image, where C(0) = S(0), C(k) = S(x - kx/L), and so on. The required number of masks ensures the preservation of texture details regardless of the orientation of the image, providing anti-rotation properties, meaning the same processing result is achieved regardless of the position of the texture on the image.

Software implementation

The software implementation is carried out using the Python programming language [12]. To simplify the implementation, ready-made library functions are used. For image processing, image reading and writing functions are provided by the OpenCV library [13]. The image processing utilizes the scipy [14] and numpy libraries. The step-by-step algorithm for improving the texture using the Atangana-Baleanu fractional differential will proceed as follows:

1. The MRI image is read in grayscale. The code for reading the image is shown in Fig. 2.

```python
image = cv2.imread(input_image_path, cv2.IMREAD_GRAYSCALE)
```

Fig. 2. The code for reading the image.

2. Based on Fig. 1, eight matrices W1-W8 are created. The coefficients for the masks are calculated using formula (12). Fig. 3 shows the code for creating masks W1-W8, with input parameters being the mask size – L and v – the order of the fractional derivative.

```python
def create_masks():
    coefficients = create_coefficients(L, v)
    W1 = util.create_matrix_with_column_results(coefficients)
    W2 = util.create_matrix_with_row_results(coefficients)
    W3 = util.create_matrix_with_column_results(coefficients, invert_results: False)
    W4 = util.create_matrix_with_row_results(coefficients, invert_results: False)

    W5 = util.create_diagonal_matrix(coefficients, corner: "top-right")
    W6 = util.create_diagonal_matrix(coefficients, corner: "bottom-left")
    W7 = util.create_diagonal_matrix(coefficients, corner: "top-left")
    W8 = util.create_diagonal_matrix(coefficients, corner: "bottom-right")

    masks_array = [W1, W2, W3, W4, W5, W6, W7, W8]
    return masks_array
```

Fig. 3. The function for creating eight masks.

3. The image is processed using a convolution operation. The convolution of the original image with each of the eight masks W1-W8 is performed using the convolution function from the scipy library. As a result, eight different images are obtained, each corresponding to the enhancement of texture in one of the directions. The corresponding code is shown in Fig.4.

```python
def convolution_operation(image, masks_array):
    convolved_results = []
    for mask in masks_array:
        convolved_image = convolve2d(image, mask, mode='same')
        convolved_results.append(convolved_image)
    return convolved_results
```

Fig. 4. The convolution operation function

4. At this stage, all the obtained images are combined into one, and then pixel normalization is performed. The corresponding code is shown in Fig.5.

```python
def results_concatenation(convolved_results):
    coefficients = create_coefficients(L, v)
    results_sum = np.sum(convolved_results, axis=0)
    normalization_value = np.sum(coefficients) * 8
    result = results_sum / normalization_value
    return result
```

Fig. 5. Concatenation function

5. The obtained enhanced image is saved to the disk as a separate file, Fig.6.

```python
cv2.imwrite(output_image_path, result)
```

**Fig. 6.** The code for writing the image

When working with medical data, it is important to choose the input set correctly, as it affects the accuracy of the study. One of the main problems is access to medical images due to their confidentiality, as

they contain personal information protected by laws. This limits the possibility of using a wide range of images and requires anonymized datasets. Another important issue is image quality. Low-resolution images or distortions can complicate texture analysis and lead to inaccurate results. Therefore, it is important to use high-quality images that adequately reflect the structures for enhancement.

In this study, an anonymized dataset from an open source [15] containing several hundred MRI images of the brain in jpg format was used. This dataset was chosen to maintain patient confidentiality while still obtaining sufficiently diverse data for testing the algorithm. The images have a high resolution (512x512 pixels), which allows for accurate analysis and processing of texture features.
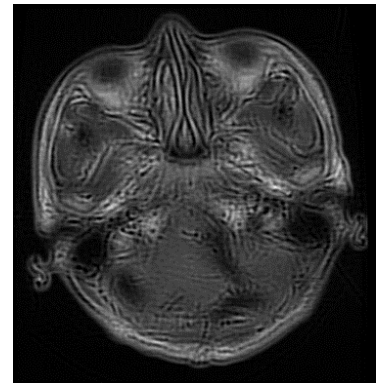
Results and Discussion

In this section, the results of the algorithm described above will be discussed. The algorithm based on fractal coefficients was executed for the range $v = [0,1;0.9]$, with the size of the applied masks $L = 7$.
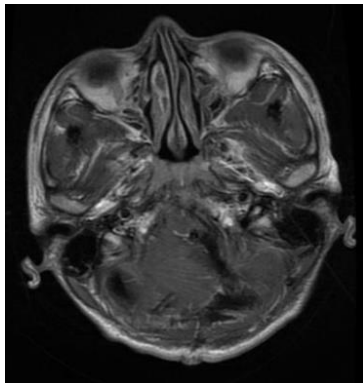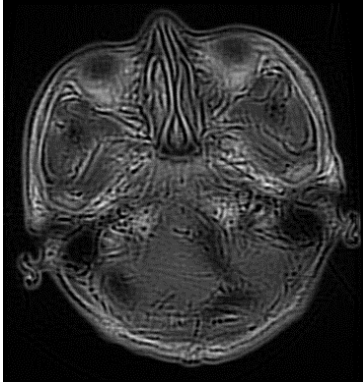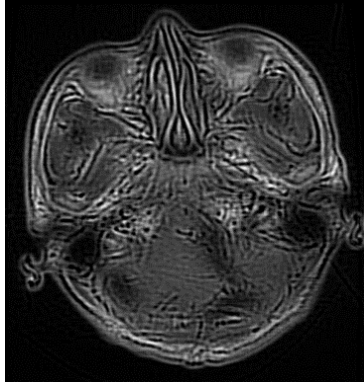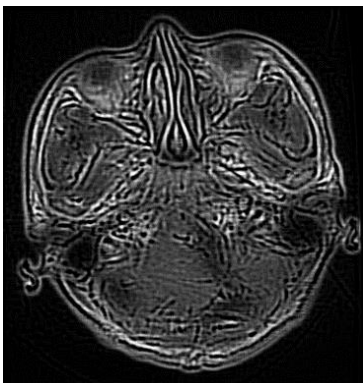

a)
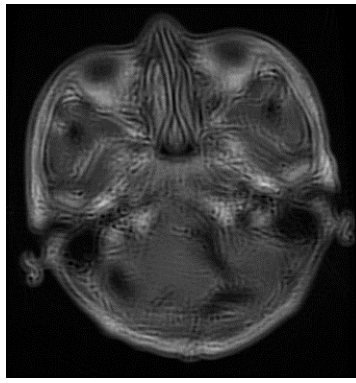
b)

c)

d)

e)

f)

g)

h)

i)

Fig. 7. MRI of the brain enhanced using the algorithm based on the ABC fractal differential coefficients: (a) original image, (b) v = 0.1, (c) v = 0.2, (d) v = 0.3, (e) v = 0.4, (f) v = 0.5, (g) v = 0.6, (h) v = 0.7, (i) v = 0.8, (j) v = 0.9

j)

According to Fig. 7, the images that underwent processing to enhance texture definition using a mask based on fractal differential coefficients demonstrate a gradual intensification of details and edges as the value of v increases. At the early stages (b), (c), (d), the changes are minimal: the texture barely differs from the original (a), and fine elements are only slightly accentuated. However, as the images progress to (e), (f), (g), a more noticeable emphasis on structural details becomes evident, particularly in the soft tissue areas and contours. The fractal effect becomes more pronounced, contributing to the increased contrast of these elements. In images (h) and (i), there is a significant enhancement of high-frequency components, allowing for clearer representation of fine structures, while low-frequency elements are slightly muted. The most pronounced changes are observed in image (j), where the texture and details are maximally highlighted, giving the image a relief effect, although this may create a sense of excessive sharpness.

The image with index (b) stands out with the softest appearance and minimal interference with the texture. As the images progress to higher values of v (from 0.1 to 0.9), there is a gradual increase in contrast at the structural boundaries, indicating a systematic enhancement of the texture elements. This dynamic suggests that the fractal differential coefficients are changing, leading to a gradual increase in detailing and clarity of the contours.

The fractal differential demonstrates its effectiveness in enhancing texture while preserving important anatomical structures. Even in images with strong enhancement (h), (i), the main brain contours remain clear, which is a critical aspect of medical imaging.

In particular, the masks based on the fractal differential are highly effective in enhancing high-frequency components, such as fine edges and microstructures, while maintaining a significant portion of the information from low-frequency regions, which correspond to smooth surfaces and large structures. However, in image (i), it is evident that excessive enhancement can lead to an effect of "over-saturation" of the edges, which may negatively impact the perception of details and the overall quality of the visualization.

Parameters comparison

For numerical comparison of images, we will use the Gray-Level Co-Occurrence Matrix (GLCM) [16]. GLCM is a matrix used for image texture analysis. It reflects the frequency with which pairs of pixels with specific intensity values appear adjacent to each other at a specified distance and in a given direction. This method allows us to evaluate the spatial relationships between pixels and highlight the texture characteristics of an image. GLCM is widely applied in various fields such as medical imaging, remote sensing, and material analysis, as it provides a rich set of statistical features for texture classification. We will construct the GLCM matrix with the following parameters: the pixel distance is set to 5, and the angles are 0, 45, 90, and 135 degrees. After constructing the GLCM, the following numerical parameters can be extracted: contrast, correlation, energy, and homogeneity.

Contrast measures the difference in intensities between adjacent pixels. High contrast indicates the presence of sharp changes between pixel intensities, which is characteristic of images with clear edges and

defined details. Low contrast, on the other hand, suggests a more uniform texture without abrupt brightness variations.

$$contrast = \sum_{i,j} (i-j)^2 P(i,j), \tag{15}$$

where, P(i,j) the coefficient of the GLCM matrix, i,j – are the indexes of matrix P.

Correlation - reflects the dependency between the intensities of neighboring pixels. High correlation indicates a strong relationship between pixel intensities, which is typical for regular or repetitive textures. Low correlation suggests less regularity or a random distribution of intensities.

$$correlation = \sum_{i,j} \frac{(i-\mu_i)(j-\mu_j)p(i,j)}{\sigma_i \sigma_j}, \tag{16}$$

$$\sigma = \sqrt{\frac{1}{n}\sum_{i=1}^{n}(p(i,j)-\mu)^2}, \tag{17}$$

where, P(i,j) the coefficient of the GLCM matrix, i,j – are the indexes of matrix P, σ_i i σ_j – standard deviations are calculated using the formula (17).

Energy characterizes the degree of texture repetitiveness. A high energy value indicates a uniform, regular texture where pixel values frequently repeat. Low energy means a more complex or chaotic image structure.

$$energy = \sum_{i,j} P(i,j)^2, \tag{18}$$

Homogeneity shows how similar the intensities of neighboring pixels are. High homogeneity indicates that the pixels have similar values, which is characteristic of uniform textures. Low homogeneity means the pixel intensities differ significantly, indicating a more complex, heterogeneous texture.
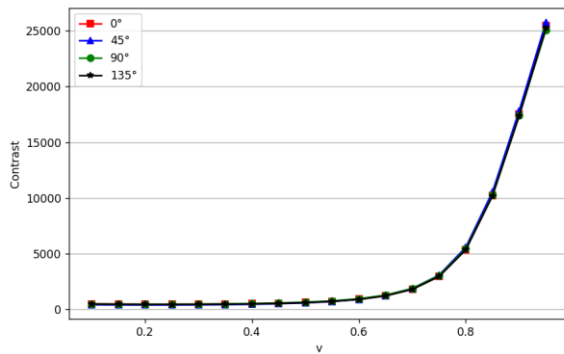
$$h = \sum_{i,j} \frac{p(i,j)}{\sigma_i \sigma_j}, \tag{19}$$

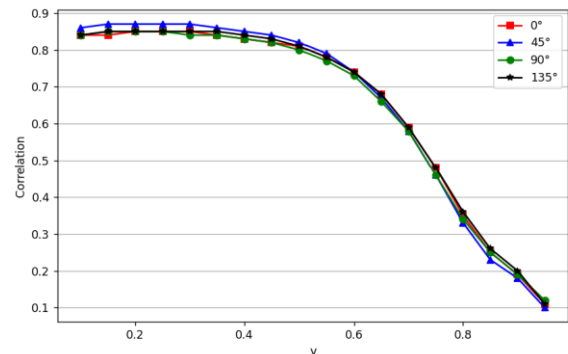Table 1 presents the values of the gray-level co-occurrence matrix for different angles of the original image.

Table 1

The values of the analytical data of the gray-level co-occurrence matrix for the original image.

Angle	0°	45°	90°	135°
Contrast	861.98	772.43	827.35	853.03
Correlation	0.76	0.78	0.77	0.76
Energy	0.07	0.07	0.07	0.07
Homogeneity	0.23	0.24	0.25	0.23

a)   b)

c)   d)
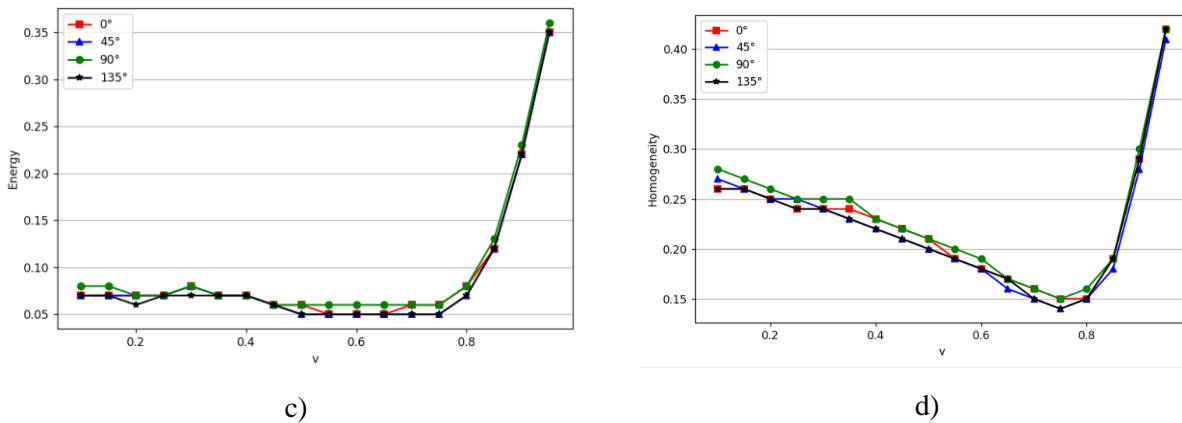
Fig. 8. The graphs of the values of contrast (a), correlation (b), energy (c), and homogeneity (d) for four angles depending on the parameter v.

In Fig.8, the relationship between contrast (a), correlation (b), energy (c), and homogeneity (d) with the fractional derivative parameter v is shown for four angles (0°, 45°, 90°, and 135°). The curves demonstrate a similar trend for all texture features, suggesting that the changes in contrast, correlation, energy, and homogeneity occur uniformly across all directions.

The graph shows that contrast increases as the value of v rises. Up to v = 0.6, all curves remain close to each other, and the contrast for all orientations stays relatively stable and low. However, after v = 0.6, a sharp rise in contrast is observed, especially when v ≥ 0.8. This indicates that at low values of the fractional derivative, the effect of the fractal filter is minimal, while higher values significantly enhance contrast. Overall, the graph suggests that the fractal filter is effective for boosting image contrast at higher v values, contributing to a better detection of textures and edges in the image.

Correlation starts high for all orientations at low v values and gradually decreases as v increases. Up to v = 0.6, correlation remains stable and nearly identical across all angles (0°, 45°, 90°, 135°), indicating that the fractal filter has a minimal effect on correlation at low fractional derivative values. After v = 0.6, however, correlation starts to drop rapidly, with the largest decrease at v ≥ 0.8, where correlation falls to around 0.1. This suggests that at higher v values, the fractal filter significantly reduces the level of correlation between neighboring pixels. The decrease in correlation indicates a reduction in the regularity and an increase in the complexity of the image texture, which is helpful for tasks like texture or edge detection.

In graph (c), the energy dependence on the value of v for several orientations (0°, 45°, 90°, 135°) is shown. For v = 0.6, the energy remains stable and nearly unchanged for all orientations, indicating minimal impact. However, at v ≥ 0.7, the energy begins to rise sharply, especially towards the end of the graph, where it increases significantly for all orientations. Despite the different angles, the overall trend is similar: initially, the energy remains stable and then increases at higher v values. This suggests the presence of complex structures, sharp intensity changes, or textured areas that become more noticeable due to the effect of the mask.

The graph (d) also shows the dependence of homogeneity on the value of v for several orientations (0°, 45°, 90°, 135°). For v = 0.6, homogeneity gradually decreases but remains stable across all orientations, indicating minor changes. However, at v ≥ 0.8, a sharp increase in homogeneity is observed, especially towards the end of the graph, where this parameter significantly rises for all orientations. Despite the different angles, the general trend is similar: initially, homogeneity decreases, and then it sharply increases at higher v values. This indicates that at large values of the parameter v, the image becomes more homogeneous, which is related to the smoothing of textures or a reduction in sharp changes between areas.

Comparison with other algorithms

As a result of the above comparisons, it was shown that images enhanced using the fractal derivative-based algorithm effectively enhance texture, specifically strengthening high-frequency areas while preserving low-frequency ones. This section presents a comparison of this algorithm with other typical texture enhancement algorithms, as well as with the algorithm based on the fractal differential of the Grünwald-Letnikov derivative. The typical algorithms include: a nonlinear image enhancement algorithm based on the Laplace transform [1], the wavelet algorithm [2], and the Sobel algorithm [3].

a)   b)   c)

d)   e)   f)
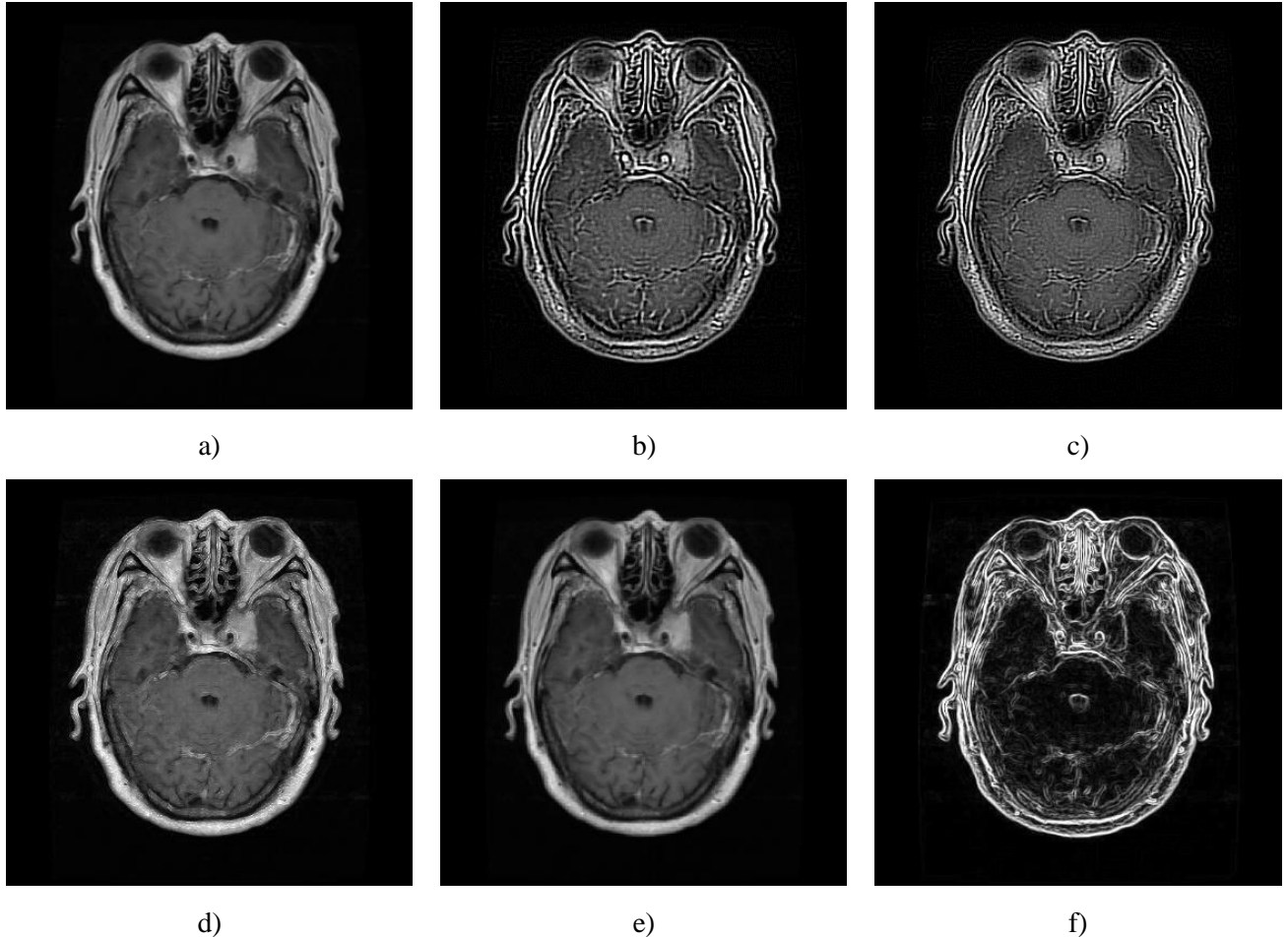
Fig. 9. MRI of the brain (a) original image, (b) enhanced with ABC fractional derivative 0.7, (c) enhanced with GL fractional derivative of order 0.7, (d) enhanced using the nonlinear algorithm based on the Laplace pyramid transform, (e) enhanced using the wavelet algorithm, (f) enhanced using the Sobel algorithm.

In Fig. 9, MRI images of the brain are shown. Image (a) is the original MRI without any processing. This is the initial image, where the main anatomical structures of the brain, fine details, and boundaries between tissues are visible. In image (b), the filter based on the ABC fractional derivative with parameter v = 0.7 is applied. This filter enhances contrast and highlights fine textural features of the brain tissue, emphasizing the boundaries between different structures. The algorithm sharpens the contours, making them clearer, which allows for better differentiation of various brain areas. The areas between the contours retain their color and remain unchanged. Image (c) is also enhanced using a fractional derivative, but this time the GL algorithm is applied with the same parameter v = 0.7. Visually, the same effects as in algorithm (b) are noticeable. The areas between the contours remain, but the contours are not as clearly defined as in image (b). Image (d) demonstrates enhancement using the nonlinear algorithm based on the Laplace pyramid transform. This algorithm provides a multi-layered representation of the image, enabling the highlighting of both global and local features. In reality, as seen, fine textures are not as well emphasized as with the fractional operator-based algorithms. In image (e), the wavelet algorithm is used to

enhance the texture. The wavelet transform simultaneously highlights both fine and large structures while preserving information about all frequency levels of the image. In image (e), it can be seen that the image has become more contrasty, but the boundaries of the areas are not as strongly highlighted, as well as the fine structures. The last image, (f), is enhanced using the Sobel algorithm, which specializes in edge detection. This method identifies sharp intensity changes between pixels, which effectively emphasizes contours and boundaries between different brain tissues. The disadvantage of this algorithm, as seen in image (f), is the complete loss of information about the large gray areas between the contours. These areas simply become black, leading to a loss of valuable information for doctors.

Comparing the enhanced images in Fig. 9, it can be concluded that the algorithms based on fractional operators performed the best in the task of texture enhancement, specifically in highlighting edges while preserving the gray areas.

Next, for a numerical evaluation of the enhancement quality, comparisons of the information entropy and the average gradient of images (b) and (c) are performed.

Information entropy [17] is a measure of how unpredictable or diverse the data is. It shows how much information is contained in the data and how difficult it is to accurately transmit or understand them. If the entropy is high, it means there are many variations in the data, and they are less organized. High entropy values indicate that the data are difficult to predict and that the system they describe is more complex or chaotic. The formula for information entropy is:

$$H(x) = \sum_{i=1}^{n} p(x_i) \log_2 p(x_i), \tag{20}$$

From formula (20), H(X) represents the value of the information entropy, $p(x_i)$ is the probability of occurrence of event x_i, and n is the number of unique pixel values that occur. The value of information entropy corresponds to the complexity and chaotic nature of the image.

The average gradient [17] is calculated as the average value of the sum of all pixel values in the image. It measures the rate of change in pixel intensity, which corresponds to the sharpness and contrast of the image.

Table 2

Numerical Comparison of Algorithms

Image	Information entropy	Average gradient
(b)	5.27	38.705
(c)	5.264	38.187

Table 2 shows the parameters of information entropy and average gradient for the images from Fig. 4 (b) and (c). The image enhanced using the fractal differential ABC shows higher values of information entropy and average gradient. This indicates that image (b) contains less organized, more chaotic data and is more complex. Regarding the high gradient value for image (b), it is also higher, meaning the image has greater contrast and sharpness compared to image (c).

Conclusions

The algorithm based on the Atangana-Baleanu fractal operator has proven effective in enhancing the textures of medical MRI images. Visual comparisons confirm that the enhanced images have better contrast, making them appear more expressive and clearer. The results of numerical comparisons show changes in numerical parameters, specifically correlation, energy, and homogeneity. These changes indicate that the enhanced images have become less homogeneous, more complex, and more contrasted. Therefore, the results of comparisons and numerical indicators suggest that this algorithm indeed improves the quality and informativeness of MRI images.

The image processing results indicate that the numerical approximation method using finite differences for the ABC fractal differential has proven effective. The approximation coefficients can be used across the entire range of values v = [0.1; 0.9].

Comparisons show that the algorithm based on the ABC fractal operator yields better texture processing results than typical image enhancement methods. Additionally, numerical comparisons of information entropy and average gradient parameters highlight its advantages over the YiFePu2 algorithm in these parameters.

The study confirmed the relevance of using the Atangana-Baleanu fractal derivative algorithm for processing medical MRI images. Specifically, the properties of the fractal differential nonlinearly enhance the frequency components of the image. Further research in this field remains relevant.

References

[1] J. K. Author, "Title of chapter in the book", in Title of the Published Book, xth ed. City of Publisher, Country if not USA: Abbrev. of Publisher, year, chapter x, section x, pp. xxx–xxx.

[2] Sobel, Irwin & Feldman, Gary. (1973). A 3×3 isotropic gradient operator for image processing. Pattern Classification and Scene Analysis. 271-272.

[3] Prewitt, J. M. S. "Object Enhancement and Extraction." In Picture Processing and Psychopictorics, edited by B. S. Lipkin and A. Rosenfeld, 75-149. New York: Academic Press, 1970.

[4] Marr, D., and E. Hildreth. "Theory of Edge Detection." Proceedings of the Royal Society of London. Series B, Biological Sciences 207, no. 1167 (1980): 187-217.

[5] Y. -F. Pu, J. -L. Zhou and X. Yuan, "Fractional Differential Mask: A Fractional Differential-Based Approach for Multiscale Texture Enhancement," in IEEE Transactions on Image Processing, vol. 19, no. 2, pp. 491-511, Feb. 2010, doi: 10.1109/TIP.2009.2035980.

[6] Van Rossum, G., and F. L. Drake Jr. *Python Reference Manual*. PythonLabs, 2001.

[7] Virtanen, P., R. Gommers, T.E. Oliphant, et al. "SciPy 1.0: Fundamental Algorithms for Scientific Computing in Python." *Nature Methods*, 17, 261-272 (2020). DOI: 10.1038/s41592-019-0686-2

[8] Bradski, G. "The OpenCV Library." *Dr. Dobb's Journal of Software Tools*, 2000.

[9] R. E. Twogood and F. G. Sommer, "Digital Image Processing," in IEEE Transactions on Nuclear Science, vol. 29, no. 3, pp. 1075-1086, June 1982, doi: 10.1109/TNS.1982.4336327.

[10] https://www.kaggle.com/datasets/navoneel/brain-mri-images-for-brain-tumor-detection/data

[11] Haralick, R.M., Shanmugam, K., and Dinstein, I. "Textural Features for Image Classification." *IEEE Transactions on Systems, Man, and Cybernetics*, vol. SMC-3, no. 6, 1973, pp. 610-621.

[12] Greenspan, H., Anderson, C. H., and Akber, S. "Image enhancement by nonlinear extrapolation in frequency space." *IEEE Transactions on Image Processing*, vol. 9, no. 6, pp. 1035–1048, Jun. 2000.

[13] Dippel, S., Stahl, M., Wiemker, R., and Blaffert, T. "Multiscale contrast enhancement for radiographies: Laplacian pyramid versus fast wavelet transform." *IEEE Transactions on Medical Imaging*, vol. 21, no. 4, pp. 343–353, Apr. 2002.

[14] Shannon, C. E. (1948). A Mathematical Theory of Communication. Bell System Technical Journal, 27(3), 379-423, 623-656.

[15] Paris, S., Hasler, D., and Morel, J.M. "A Fast Algorithm for the Computation of the Exact Euclidean Distance Transform." *IEEE Transactions on Image Processing*, vol. 21, no. 1, pp. 22–30, Jan. 2012.

[16] Manokhin D., Sokolovskyy Ya., "Intracranial Hemorrhage Segmentation Using Neural Network and Riesz Fractional Order Derivative-based Texture Enhancement", Computer Design Systems. Theory and Practice, 2024; Volume 6, Number 1:1-16, https://doi.org/10.23939/cds2024.01.001

[17] Massopust, Peter. (1997). Fractal Functions and their Applications. Chaos Solitons & Fractals. 8. 171-190. 10.1016/S0960-0779(96)00047-1.

Володимир Березюк[1], Ярослав Соколовський[2]

[1] Кафедра комп'ютерних наук, Національний лісотехнічний університет України, вул. Генерала Чупринки, Львів, Україна, E-mail: volodymy.berezyuk@nltu.edu.ua, ORCID 0009-0001-6930-4235

[2] Кафедра систем автоматизованого проектування, Національний університет "Львівська політехніка", вул. С. Бандери 12, Львів, Україна, E-mail: yaroslav.i.sokolovskyi@lpnu.ua, ORCID 0000-0003-4866-2575

ПОКРАЩЕННЯ МЕДИЧНИХ МРТ ЗОБРАЖЕНЬ НА ПІДСТАВІ ФРАКТАЛЬНОГО ОПЕРАТОРА АТАНАГАНА-БАЛЕАНУ

Enhancement of Medical MRI Images Based on the Atanagan-Baleanu Fractal Operator

Анотація. У даній статті описується використання фрактального оператора Атангана-Белеану для задачі покращення текстур медичних МРТ зображень. Детально наводиться математичний апарат фрактального диференціала Атангана-Белеано. Розглядається числовий підхід обчислення фтрактального диференціала за допомогою методу скінченних різниць. На основі апроксимованого розв'язку, знаходяться коефіцієнти апроксимації. Коефіцієнти апроксимації використовуються для створення восьми різнонаправлених масок, які застосовуються як фільтри для просторової обробки зображень в різних напрямках. Створено і описано відповідний алгоритм застосування фрактальних масок. Проведено порівняння отриманих результатів роботи алгоритму обробки медичних зображень. Проведено дослідження зміни параметрів зображень в наслідок роботи алгоритму покращення зображень. А також проводиться порівняння роботи алгоритму з іншими алгоритмами для покращення текстур.

Ключові слова: Магнітно-резонансна томографія (МРТ), фрактальний оператор Атангана-Белеану, покращення зображень, Python.